

Solid-State ^1H MAS NMR Characterization of γ -Alumina and Modified γ -Aluminas

E. C. DeCanio,* J. C. Edwards,* and J. W. Bruno†

*Texaco Research and Development Department, Beacon, New York 12508; and †Wesleyan University, Middletown, Connecticut 06459

Received May 24, 1993; revised February 10, 1994

^1H single pulse MAS and CPMG T_2 /CSA-filter NMR experiments have been performed in order to characterize the hydroxyl structure of γ -alumina, as well as fluoride- and phosphate-modified γ -alumina materials. We have shown that problems associated with the strong homonuclear dipole–dipole interactions between protons of neighboring OH groups can be overcome by isotopic dilution of the alumina surface protons by deuterium exchange. Partially deuterated γ -alumina yields resonances at around -0.3 , 0.3 , 1.5 , 2.4 , 4.0 , 5.0 , 6.5 , 7.1 , and 7.8 ppm. CPMG T_2 /CSA-filter NMR experiments performed on alumina calcined at 700°C show that five different types of hydroxyl groups are present. CPMG T_2 /CSA-filter NMR of deuterated $\text{F}/\text{Al}_2\text{O}_3$ produces a resonance at 11.5 ppm in addition to a range of resonances between -0.2 and 7 ppm. NMR data for calcined $\text{P}/\text{Al}_2\text{O}_3$ and $\text{P-Mo}(12)/\text{Al}_2\text{O}_3$ (wt% P = 0.0 – 10.0) show that polymeric orthophosphates produce a resonance at 3.4 ppm, while the monomeric orthophosphate species gives rise to a resonance at 1.2 ppm. © 1994 Academic Press, Inc.

INTRODUCTION

γ - Al_2O_3 is one of the most commonly used supports in commercial heterogeneous catalysts. It possesses a defect spinel lattice structure which is terminated by surface hydroxyl groups (1–3). These hydroxyl groups play an important role in determining the surface chemistry of the resulting alumina-based catalysts. During the preparation of supported metal oxide catalysts, the metal species interact with the alumina hydroxyl groups to produce dispersed metal oxide phases (4–6). Changing the nature of the hydroxyl groups by the addition of modifiers, such as phosphate or sulfate, has been shown to affect the structure and dispersion of the metal oxide species (7, 8). Additionally, new environmental regulations regarding reformulation of petroleum products are heightening interest in the use of modified aluminas as acid catalysts (9–11). Thus, there is a need to be able to characterize the hydroxyl structure of alumina and other oxide supports.

The technique which is used most extensively to study the hydroxyl structure of Al_2O_3 systems is FTIR. Data

from IR studies of the hydroxyl regions of $\text{Mo}/\text{Al}_2\text{O}_3$ (12), $\text{PO}_4/\text{Al}_2\text{O}_3$ (8), and $\text{F}/\text{Al}_2\text{O}_3$ (13) catalysts have been published. Unfortunately, poor resolution of the IR bands in the 4000 – 3200 cm^{-1} range often makes it impossible to determine unequivocally whether new hydroxyl groups have formed (giving rise to new bands), or if existing hydroxyl groups have been modified by the interaction with promoter species, thus causing the hydroxyl stretching band to shift (14).

Another technique which is being used increasingly to gain information concerning the hydroxyl structure of heterogeneous materials is solid-state ^1H magic angle spinning (MAS) NMR (15–25). In the ^1H MAS NMR experiment the chemical shift position of the observed proton resonance yields information about the acid strength of the hydroxyl group, while the intensity of the resonance can give a semiquantitative measure of the relative numbers of the different types of OH groups (17). ^1H MAS NMR has been used extensively to study amorphous Al_2O_3 – SiO_2 , SiO_2 , and zeolitic (18) materials, but there have been very few attempts to utilize ^1H NMR to study the hydroxyl structure of oxide supported catalysts. Mastikhin and co-workers have reported ^1H NMR studies of $\text{Mo}/\text{Al}_2\text{O}_3$ (19), anatase (20), aluminophosphates, and TiO_2 - and SnO_2 -supported V_2O_5 (21). Most of these previous studies involved MAS of sealed samples that necessitated the use of low MAS spinning speeds, which leads to the presence of spinning side bands in the 9 – 15 ppm region; this precludes the observation of any resonances due to hydroxyl groups that may arise in that shift range. In this work we have also studied the reproducibility obtained while running the ^1H spectra in standard MAS rotors without recourse to vacuum-line sealing of samples in glass ampoules.

In this paper, we report solid-state ^1H MAS data for γ -aluminas which have been subjected to various pretreatments. We show that reduction of the sample in a deuterium atmosphere at 400°C allows one to characterize acidic hydroxyl groups not previously observed for γ -alumina. We have identified several types of hydroxyl groups present on an alumina sample calcined at 700°C ,

and can distinguish these from physisorbed water or water adsorbed onto Lewis acid sites.

In addition, we report NMR data for a series of deuterium-reduced $\text{F}/\text{Al}_2\text{O}_3$ materials (wt% F = 0.0–10.0), and a series of $\text{P}/\text{Al}_2\text{O}_3$ and $\text{P-Mo(12)}/\text{Al}_2\text{O}_3$ (wt% P = 0.0–10.0) materials in their calcined state. Again, we were able to characterize more fully the hydroxyl structure of these materials. The results presented here demonstrate the potential of solid-state ^1H MAS NMR to characterize fully the hydroxyl structure of heterogeneous catalysts.

EXPERIMENTAL

Sample Preparation

The γ -alumina used was Norton (6375C, 20/40 mesh) with a surface area of $221 \text{ m}^2 \text{ g}^{-1}$ and a pore volume of 1.4 ml g^{-1} . Elemental analysis revealed the presence of no impurities. The experimental details for the preparation of the $\text{P}/\text{Al}_2\text{O}_3$, $\text{P-Mo(12)}/\text{Al}_2\text{O}_3$, and $\text{F}/\text{Al}_2\text{O}_3$ samples have been given previously (8, 13). The $\text{P}/\text{Al}_2\text{O}_3$ and $\text{P-Mo(12)}/\text{Al}_2\text{O}_3$ samples were calcined at 500°C under flowing air for 5 hr. The calcined samples were then transferred, within 15 sec, to the MAS rotor in a zero-humidity atmosphere, and the NMR spectrum was obtained. Tight fitting Kel-F end caps were used to prevent sample hydration during the spectrum accumulation. Spectra run before and after the experiment confirmed that no "in-rotor" hydration occurred in any of the experiments. $\text{F}/\text{Al}_2\text{O}_3$ samples were reduced at 400°C under a deuterium atmosphere ($40 \text{ cm}^3/\text{min}$) for 1 hr. The calcined or reduced samples were then quickly transferred to the rotors in the same manner. All spectra were found to be reproducible when samples were loaded in this manner.

^1H NMR Procedure

The spectra were obtained on a Varian VXR-300 and a Varian Unity-300 NMR Spectrometer operating at 300 MHz for ^1H , utilizing MAS at speeds of 7–8 kHz. A Doty Scientific 5-mm CRAMPS probe and sapphire rotors with Kel-F end caps were used. The acquisition time was 0.08 sec; relaxation delay was 0.5 sec (a 20° tip angle was used for the single pulse (SP) experiments). The reference used was TMS (0 ppm). A modification of the Carr–Purcell–Meiboom–Gill (CPMG) sequence was used in order to perform T_2/CSA -filter experiments (17, 22–24). This sequence consists of a 90° pulse followed by a variable length train of 180° pulses as follows:

$$\pi/2-t-(-\pi)_n-t\text{-Acquire.}$$

This echo train allows the loss of spin coherence in the transverse plane of the rotating frame to be repeatedly refocused. However, with increasing echo train length,

different components of magnetization are lost. By varying the length of the echo train, and making no attempt to synchronize sample rotation with the echo delay, t , one can effectively observe only those protons with long transverse relaxation times (T_2), and small values of chemical shielding anisotropy (CSA). Thus, one is spectrally filtering the data based on the T_2 's and CSA's of the various hydroxyls. A $2.5\text{-}\mu\text{sec}$ 90° pulse was used in these T_2/CSA -filter experiments. This experiment has the effect of increasing the resolution of the NMR data, as species with long T_2 relaxation times have inherently narrower resonance lines. Thus, one observes details which are often partially or completely obscured in the SP/MAS spectra. In all cases background spectra, representing around 20–30% of the total observed signal, were obtained and subtracted from the experimental data. This is necessary as water was not rigorously excluded from the experimental hardware.

Deconvolution of the spectrum of deuterated $\gamma\text{-Al}_2\text{O}_3$ into its individual components was performed using the Varian spectrometer software, assuming a half Lorentzian/half Gaussian component lineshape. A least-squares analysis of the "fit error" revealed that a nine-component fit gave the minimum fit error. Deconvolution was performed on this one spectrum in order to demonstrate the multicomponent nature of the observed ^1H spectra. Spectral assignments of all the ^1H spectra were made based on the observed singularities.

RESULTS AND DISCUSSION

^1H NMR Studies of γ -Alumina

The ^1H SP/MAS NMR spectrum of $\gamma\text{-Al}_2\text{O}_3$ calcined in air at 400°C is shown in Fig. 1A. It exhibits resonances at -0.4 and 2.2 ppm that have been assigned to the basic and acidic hydroxyl groups, respectively, which are formed when a small amount of moisture is adsorbed onto calcined Al_2O_3 . This spectrum is similar to previously reported ^1H NMR data of γ -alumina (19). Unfortunately, strong homonuclear dipole–dipole interactions between protons of neighboring hydroxyl groups or physisorbed water molecules cause the signals to broaden, resulting in poor resolution. One way to overcome this problem is to replace some of the surface hydrogen atoms with deuterium atoms. This will isotopically dilute the alumina surface protons, thus reducing the homonuclear dipolar interactions and giving better resolution.

The SP/MAS spectrum of deuterated γ -alumina calcined at 400°C is shown in Fig. 1B. Resonances are observed at ca. 0, 0.3, 0.9, 1.6, 2.6, 4.1, and 7.3 ppm. Additionally, we have carried out the CPMG T_2/CSA -filter experiment. In this experiment the species with shorter T_2 relaxation times, and large CSA's are not observed.

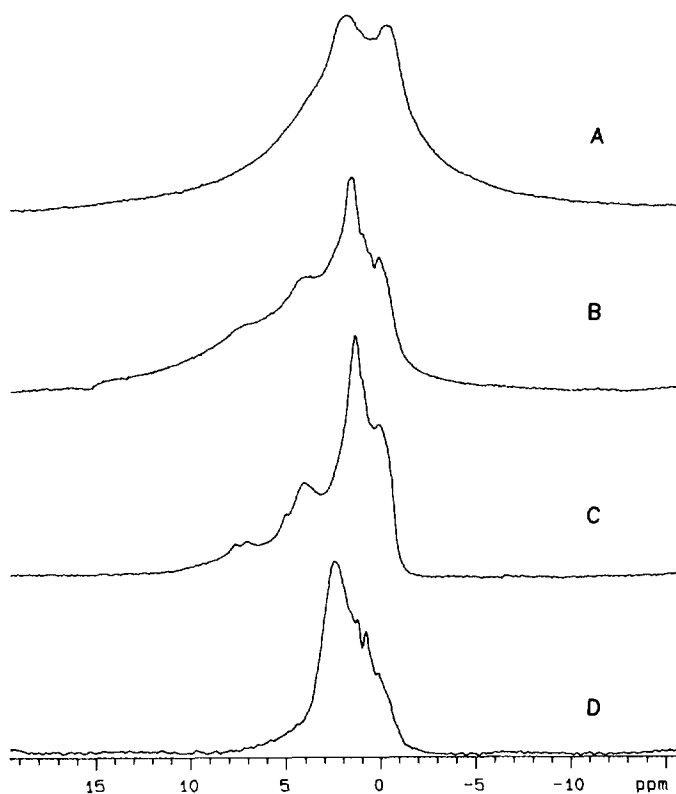


FIG. 1. Solid-state ^1H NMR spectra of γ -alumina after various pre-treatments: (A) SP/MAS after a 400°C calcination; (B) SP/MAS after a 400°C deuteration, (C) CPMG T_2 /CSA-filter after a 400°C deuteration, and (D) CPMG T_2 /CSA-filter after a 700°C calcination.

Species with shorter T_2 relaxation times (less than 1 msec) would include hydroxyls in regions that were not effectively isotopically diluted with deuterium during the reduction/calcination procedure. These hydroxyls would be subject to stronger ^1H - ^1H dipolar interactions which would reduce the T_2 relaxation times considerably compared to effectively diluted hydroxyls. Figure 1C shows the spectrum of $\gamma\text{-Al}_2\text{O}_3$ obtained using τ set at $6.1 \mu\text{sec}$ and $n = 501$. One can see that the resolution has been greatly increased, allowing the observation of three small resonances (at 5.0, 7.1, and 7.8 ppm) that are barely discernible in the SP/MAS spectrum (Fig. 1B).

Concerns over the effect of ^{27}Al - ^1H heteronuclear dipolar couplings on the multiplicity of the observed ^1H resonances are addressed by the use of the CPMG pulse sequence which effectively averages this interaction (17, 24). In combination with the partial averaging of this interaction afforded by the MAS technique, and the fact that the ^{27}Al - ^1H interaction decreases with field-strength (25), one can be confident that the resonances observed in CPMG T_2 /CSA-filter experiments, here performed at 7 T, are due to chemically distinct protons.

We have performed curve analysis on both the SP/MAS and CPMG T_2 /CSA-filter data of deuterated γ -alumina,

and the results for the CPMG T_2 /CSA-filter data are shown in Fig. 2. It can be seen that the observed ^1H lineshape results from the combination of nine Lorentzian/Gaussian resonances at -0.3 , 1.5 , 2.4 , 4.0 , and 6.5 ppm, along with additional signals of low intensity at 5.0 , 7.1 , and 7.8 ppm. This curve analysis indicates that there is a broad distribution of surface hydroxyl sites. However, due to the problems associated with curve-fitting analysis of multiple component lineshapes, we have not based any of our subsequent assignments on this type of analysis.

^1H NMR studies of zeolites and amorphous silica-aluminas have shown that resonances near 7 ppm can be attributed to strong Brønsted acid sites produced when water is adsorbed onto Lewis acid sites (26). Hunger *et al.* have shown that there is a correlation between the intensity of the 7-ppm resonance and the cumene cracking activity of silica-aluminas (26). This resonance has not been observed previously for alumina; indeed, it has been suggested that the Brønsted acid site giving rise to this signal occurs in regions of zeolites or silica-aluminas in which there is an interface between silica and alumina structures. However, the NMR data presented here clearly show the presence of a very small amount of these strong Brønsted acid sites on the pure γ -alumina surface. The signal at ca. 4.6 ppm has been assigned to hydrogen-bonded water present on the alumina surface, and the 1.2-ppm resonance to non-hydrogen-bonded, physisorbed water (27).

Much of the early work on the hydroxyl structure of γ -alumina was carried out by Peri and co-workers using FTIR spectroscopy (28-30). They observed a continual loss of surface OH groups as the calcination temperature was increased from 100 to 800°C . The IR spectrum of γ -alumina calcined at 800°C exhibits five bands in the 3700 - 3800 cm^{-1} region, showing the presence of five distinct types of OH groups. Knözinger and Ratnasamy have developed a model for the alumina surface which accounts for the presence of these five different types of hydroxyl groups, the properties of which are predominately determined by the coordination number and net electrical charge of the aluminum site (1). The proposed structures of the five sites are shown in Scheme I.

In order to assign more accurately the proton NMR resonances, we have obtained CPMG T_2 /CSA-filter NMR spectra of an alumina sample that has been calcined at 700°C (Fig. 1D). There are resonances remaining at -0.3 , 0.0 , 0.9 , 1.2 , 1.5 , and 2.4 ppm, showing that there are five distinct OH groups present, in addition to some non-hydrogen-bonded water (1.2 ppm); this is in agreement with Knözinger's model (1). It can also be seen that the 700°C calcination results in the disappearance of the previously observed resonances at 4.1 , 5.1 , 7.3 , and 7.8 ppm, and considerable reduction in the intensity of the resonance at 1.2 ppm. The loss of these resonances is expected

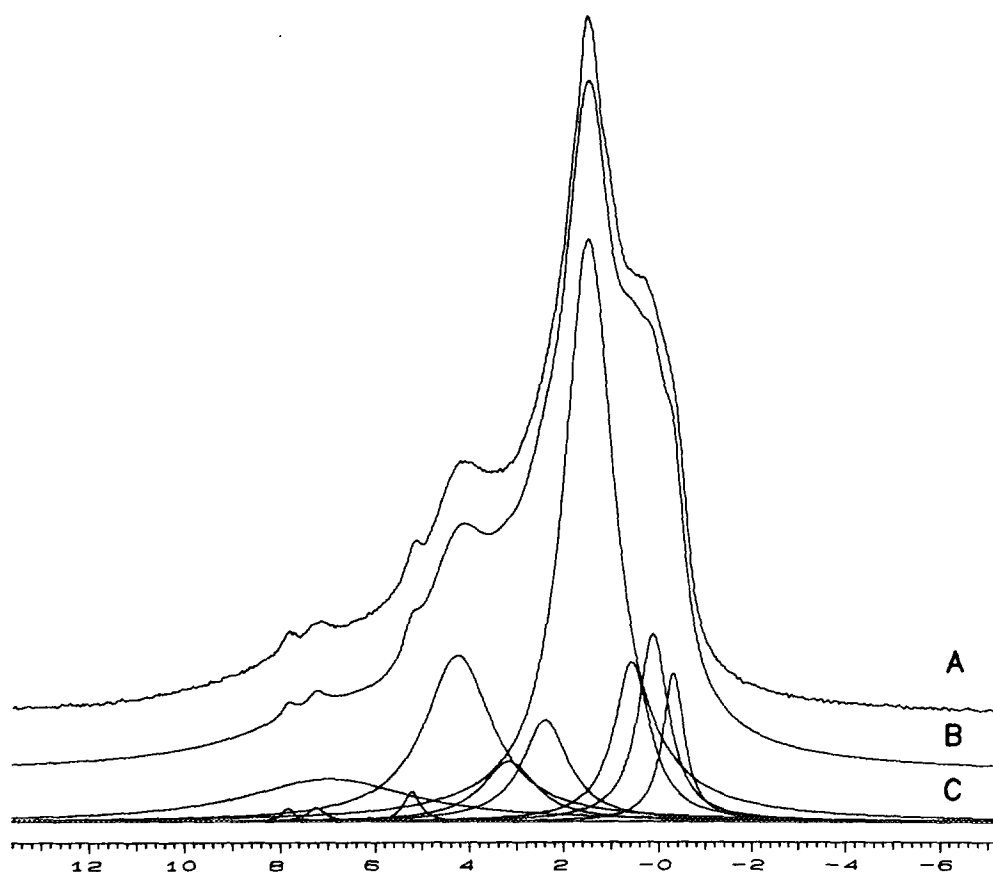


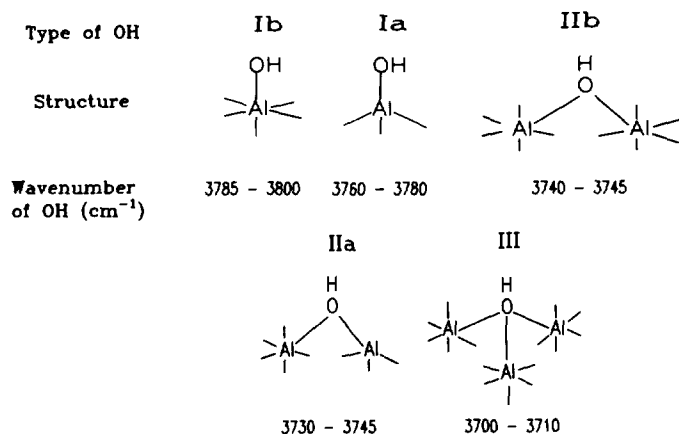
FIG. 2. Curve analysis results of the CPMG T_2 /CSA-filter ^1H NMR spectrum of deuterated γ -alumina: (A) experimentally obtained spectrum, (B) generated spectrum, and (C) deconvoluted curves.

since we have attributed them to OH groups produced when water is adsorbed onto alumina. Although we cannot make an unequivocal assignment of the -0.3 , 0.0 , 0.9 , 1.5 , and 2.4 ppm resonances, we can assign the -0.3 -ppm signal to the most basic OH group (which Knözinger has termed the Type Ib site (Scheme I)) and the resonance

at 2.4 ppm to the most acidic (Type III) group (Scheme I). Presumably, the other resonances are due to the hydroxyl groups of intermediate acid and base strengths, with the resonance at 1.2 ppm due to non-hydrogen-bonded water (1, 15, 16).

The observation that the 2.4 -ppm resonance has the highest intensity indicates that the alumina surface has a higher density of the most acidic groups. This is consistent with Pauling's electrostatic valence rule (1).

Thus, we have shown that ^1H SP/MAS and CPMG T_2 /CSA-filter characterization of partially deuterated alumina reveals information regarding the nature of the hydroxyl groups present. We have shown that these measurements are sensitive enough to observe resonances above 5 ppm previously unreported for γ -alumina.



SCHEME I. Proposed structures for the five types of hydroxyl groups on γ -alumina (1).

^1H NMR Studies of Deuterated $F/\text{Al}_2\text{O}_3$ Samples

The addition of fluoride to alumina has been shown to increase the catalytic activity of alumina for acid-catalyzed reactions such as cracking (31, 32), isomerization (33), and polymerization (34). FTIR analysis of pyridine adsorption has shown the predominant effect of adding small amounts of fluoride to Al_2O_3 is to increase the Lewis

and Brønsted acidity of the alumina; however, pyridine adsorption does not differentiate between the density and strength of the various acid sites (35).

The ^1H SP/MAS spectra for a series of partially deuterated $\text{F}/\text{Al}_2\text{O}_3$ samples in which the fluoride loading is varied from 0.0 to 10.0 are shown in Fig. 3. The $\text{F}(0)/\text{Al}_2\text{O}_3$ sample is the one discussed above, and is shown in Fig. 3A. The addition of 2 wt% F results in the loss of the signal at -0.3 ppm, the growth of signals at 4.5 and 6.8 ppm, and the appearance of a resonance at 11.5 ppm (Fig. 3B). The loss of the resonance at -0.3 ppm is due to the fact that fluoride is replacing the basic alumina hydroxyl groups (13). Increasing the fluoride loading to 5 wt% causes the continual growth of the resonances in the 2–5 ppm region and of the resonance at 6.8 ppm. At this loading, the 11.5-ppm resonance is still present. The effect of having 10 wt% F present is shown in Fig. 3C. It can be seen that the 11.5-ppm resonance is no longer visible and the overall intensity of the signals has decreased. Also apparent from Fig. 3 is a general shift of all the signals toward lower field as the fluoride loading is increased.

Hunger *et al.* have shown that if small amounts of water are adsorbed onto zeolite and amorphous silica–aluminas, the water molecules can hydrogen-bond to Brønsted acid sites, producing hydroxonium ions. The chemical shift of these hydroxonium ions was shown to be in the 8–19 ppm range (15). Thus, the appearance of the 11.5-ppm signal when fluoride is added to alumina shows the presence of a strong Brønsted acid site. The formation of this strong Brønsted acid site is due to the through-lattice inductive effect of the electronegative fluoride (32). However, the

increase in the strength of the Brønsted acid sites is accompanied by a decrease in the density of alumina hydroxyl groups due to the replacement of the OH groups with fluoride, and because of the formation of bulk phases of aluminum fluoride (13). This gives rise to the observation that the activity of fluorided catalysts for alkylation reactions is maximum at ca. 5 wt% F (32). To our knowledge, this is the first NMR characterization of the strong Brønsted acid sites resulting from the addition of fluoride to alumina.

The growth of the signals between 2 and 5 ppm and at 6.8 ppm with increasing F loading is indicative of water molecules or hydroxyl groups associated with the bulk aluminum fluoride phases that are present. Previously we have shown that three types of aluminum fluoride phases are present on the alumina surface (13); these differ in the number of water molecules around the aluminum ion ($\text{AlF}_3 \cdot n\text{H}_2\text{O}$, $n = 1-3$).

^1H NMR Studies of Calcined $\text{P}/\text{Al}_2\text{O}_3$ Samples

The presence of phosphorus in Ni–Mo/ Al_2O_3 hydro-treating catalysts has led to much research aimed at understanding the role of the phosphorus (8). Others have used NH_3 TPD to determine that the addition of phosphorus creates acid sites (36, 37), but little is known of the nature of the acid sites. The ^1H SP/MAS NMR spectra of calcined $\text{P}/\text{Al}_2\text{O}_3$ samples (where the phosphorus loading is varied from 0.0 to 10.0 wt%) are shown in Fig. 4. $\gamma\text{-Al}_2\text{O}_3$ exhibits two resonances at -0.4 and 2.2 ppm (Fig. 4A) which can be assigned to the basic and acidic hydroxyl

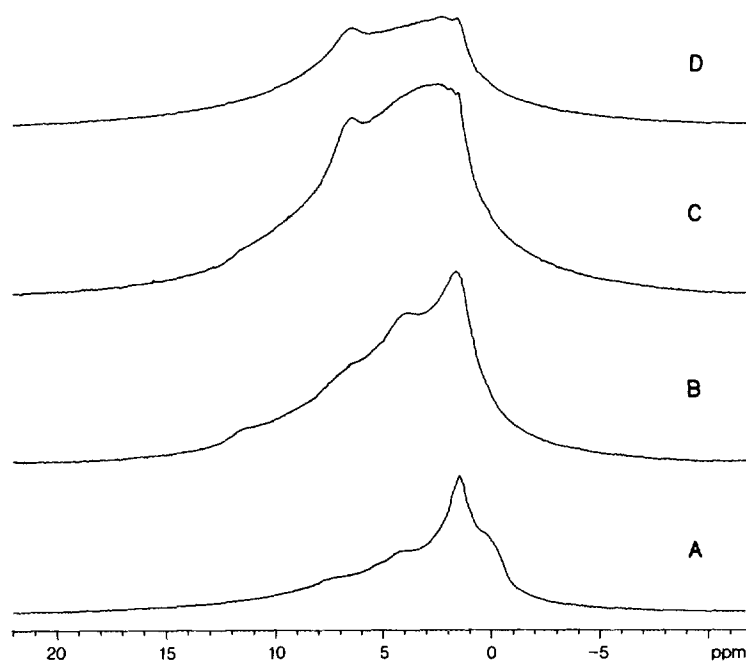


FIG. 3. ^1H SP/MAS NMR spectra of $\text{F}/\text{Al}_2\text{O}_3$ samples: (A) 0.0 wt% F, (B) 2.0 wt% F, (C) 5.0 wt% F, and (D) 10.0 wt% F.

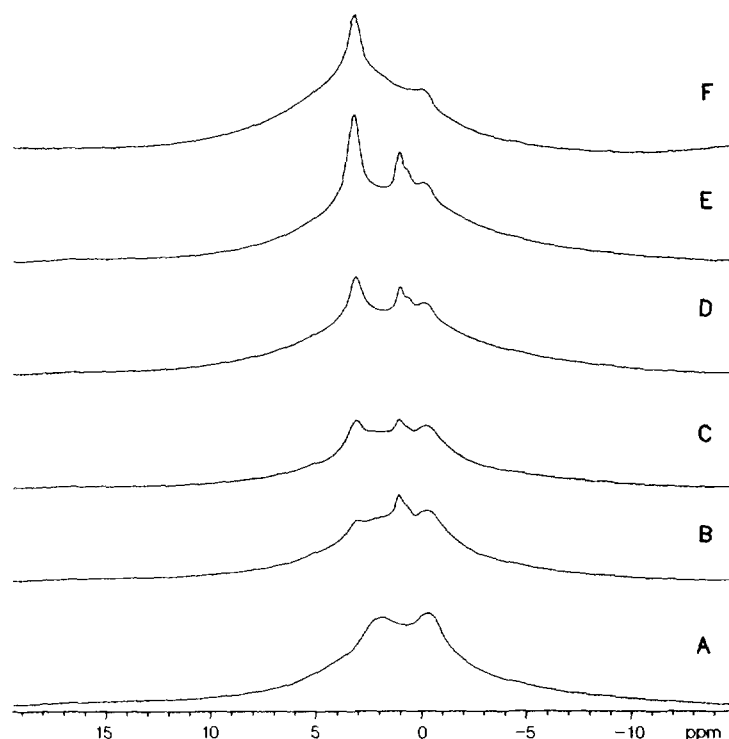


FIG. 4. SP/MAS ^1H NMR spectra of $\text{P}/\text{Al}_2\text{O}_3$ samples: (A) 0.0 wt% P, (B) 1.0 wt% P, (C) 2.0 wt% P, (D) 4.0% P, (E) 8.0 wt% P, and (F) 10.0 wt% P.

groups discussed above (18). The addition of 1.0 wt% P to the Al_2O_3 results in the appearance of three resonances at 0.6, 1.1, and 3.4 ppm, and the decrease in intensities of the resonances at -0.4 and 2.2 ppm. The intensities of the 0.6, 1.1, and 3.4 ppm resonances increase as the P loading is increased to 8.0 wt%. At 10 wt% P, the 0.6 and 1.1 ppm resonances disappear, and the intensity of the 3.4 ppm signal decreases slightly. The appearance of three signals demonstrates that there are three distinct types of OH groups present on the calcined $\text{P}/\text{Al}_2\text{O}_3$.

The ^1H SP/MAS NMR spectra of calcined $\text{P}-\text{Mo}(12)/\text{Al}_2\text{O}_3$ (wt% P = 0.0–10.0) are shown in Fig. 5. $\text{P}(0)\text{Mo}(12)/\text{Al}_2\text{O}_3$ exhibits a resonance at 2 ppm with a shoulder at 4 ppm. The fact that there is no resonance at -0.4 ppm shows that molybdate preferentially interacts with the most basic alumina hydroxyl groups (12, 38). From Fig. 5, it can be seen that the presence of phosphate gives rise to a resonance at 3.4 ppm which becomes more intense as the phosphorus loading is increased. Underlying this resonance is a broad resonance centered at ca. 4 ppm, which can be assigned to physisorbed water. Increasing the P loading to 10 wt% leads to an overall loss of intensity in the resonance at 3.4 ppm, while the broad signal at 4 ppm becomes larger.

Previous studies have shown that during the preparation of $\text{P}/\text{Al}_2\text{O}_3$ samples, phosphoric acid initially reacts with the basic Al_2O_3 hydroxyl groups; as the P loading is

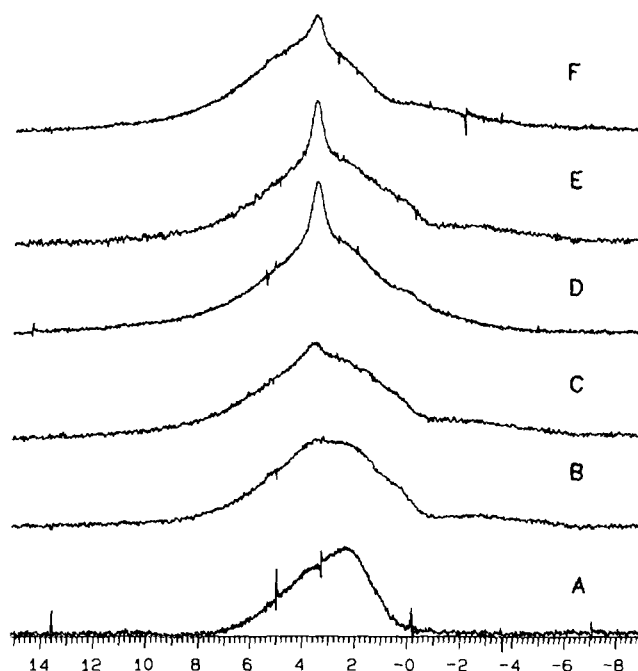


FIG. 5. SP/MAS ^1H NMR spectra of $\text{P}-\text{Mo}(12)/\text{Al}_2\text{O}_3$ samples: (A) 0.0 wt% P, (B) 0.5 wt% P, (C) 2.0 wt% P, (D) 4.0 wt% P, (E) 6.0 wt% P, and (F) 10.0 wt% P.

increased, phosphoric acid eventually reacts with the more acidic groups (8). Several types of phosphate species form on the Al_2O_3 surface of dried $\text{P}/\text{Al}_2\text{O}_3$, depending on the P loading and the pretreatment (8). At P loadings of 1 wt%, monomeric orthophosphate species form, but at higher P loadings, polymeric orthophosphates begin to form; finally, at ca. 8 wt% P, bulk aluminum phosphate results (8). The effect of calcining the $\text{P}/\text{Al}_2\text{O}_3$ is to convert some of the monomeric orthophosphates into polymeric phosphates, and to disperse the crystalline aluminum phosphate as amorphous phases on the alumina surface. Additionally, we previously showed that $\text{P}-\text{Mo}(12)/\text{Al}_2\text{O}_3$ has a greater density of polyphosphates than does the $\text{P}/\text{Al}_2\text{O}_3$, and that the presence of 12 wt% Mo causes the formation of much more aluminum phosphate (8).

The SP/MAS ^1H NMR results observed in Figs. 4 and 5 demonstrate that the addition of P to Al_2O_3 results in the creation of three types of OH groups, while the presence of P in $\text{Mo}(12)/\text{Al}_2\text{O}_3$ materials gives rise to one OH group only. Mastikhin *et al.* have observed resonances at 3.5 and 1.9 ppm for $\text{H}_3\text{PO}_4/\text{SiO}_2$ with the resonance at 3.5 assigned to SiP_2O_7 (39). We can, therefore, tentatively assign the resonances found at 3.4 ppm to the OH associated with the polymeric orthophosphate and the resonances at 1.1 and 0.6 ppm to different OH groups associated with monomeric orthophosphate groups (present on the $\text{P}/\text{Al}_2\text{O}_3$ samples only). This is also consistent with measured $\text{p}K_a$'s of phosphates (40), which indicate that polyphosphates are typically more acidic than are orthophosphates. The broad signal at 4 ppm is due to water physisorbed on to the aluminum phosphate.

The presence of two types of phosphate on the $\text{P}/\text{Al}_2\text{O}_3$ materials is also in agreement with the conclusions of Stanislaus and Morales, who have studied $\text{P}/\text{Al}_2\text{O}_3$ samples by NH_3 TPD; see (36, 37). Both researchers have found that the addition of phosphorus to Al_2O_3 decreases the number of strong acid sites but increases the number of medium and weak acid sites. The overall result is an increase in the number of acid sites, but a decrease in the number of strong acid sites necessary to catalyze coke formation and skeletal isomerization reactions (41). Our data show that these new acid sites are associated with the phosphate species, and the shifts of 3.4 and 1.1/0.6 ppm confirm that these are relatively weak acid sites.

CONCLUSIONS

We have shown that solid-state ^1H NMR can be used to reproducibly characterize the hydroxyl structure of γ -alumina and modified γ -alumina materials, without recourse to the sample sealing and vacuum line manipulations. We have shown that the problem associated with the strong homonuclear dipole-dipole interactions between protons of neighboring OH groups can be overcome

by partially exchanging protons on the alumina surface with deuterium atoms. Additionally, by carrying out CPMG T_2 /CSA-filter experiments it is possible to improve the resolution of the technique.

Some of the major conclusions of this work are:

1. By partially deuterating the γ -alumina surface, one is able to observe resonances at 7.2 and 7.8 ppm not previously observed. These resonances are attributed to strong acid sites formed when water is adsorbed on Lewis acid sites.

2. NMR of γ -alumina calcined at 700°C shows five different types of hydroxyl groups are present, in agreement with the Knözinger model (1). By comparing NMR data gathered after the different pretreatments, we are able to differentiate between these OH groups and those formed by adsorption of water.

3. The $\text{F}/\text{Al}_2\text{O}_3$ catalysts exhibit hydroxyl signals at lower shielding, which can be attributed to the through-lattice inductive effect withdrawing electron density from the surface protons.

4. For $\text{F}/\text{Al}_2\text{O}_3$, we have characterized a resonance at 11.5 ppm, showing the presence of a strong Brønsted acid site, the intensity of which was greatest at ca. 5 wt% F. A resonance resulting from the presence of an increased number of Lewis acid sites was observed at 6.8 ppm. Also, an overall loss of signal intensity was observed with increased loading due to the substitution of surface hydroxyls by fluorine. By comparing NMR data for the different fluoride loadings, we can observe the creation of strong Brønsted acid sites, the creation of Lewis acid sites, and the replacement of surface hydroxyl groups by fluoride and amorphous aluminum fluoride phases.

5. Interpretation of the NMR data for calcined $\text{P}/\text{Al}_2\text{O}_3$ and $\text{P}-\text{Mo}(12)/\text{Al}_2\text{O}_3$ shows that polymeric orthophosphates produce resonances at 3.4 ppm, while the monomeric orthophosphate species gives rise to resonances at 1.1 and 0.6 ppm.

ACKNOWLEDGMENTS

We thank Tom Scalzo for the preparation of all the samples in this study. We also thank Texaco, Inc., for permission to publish this work.

REFERENCES

1. Knözinger, H., and Ratnasamy, P., *Catal. Rev.-Sci. Eng.* **71**(1), 31 (1978).
2. Ballinger, T. H., and Yates, J. T., *Langmuir* **7**, 3041 (1991).
3. Sanchez, M. G., and Gazquez, J. L., *J. Catal.* **104**, 120 (1987).
4. Okamoto, Y., and Toshinobu, I., *J. Phys. Chem.* **92**, 7102 (1988).
5. Segawa, K., and Hall, W. K., *J. Catal.* **76**, 133 (1982).
6. Millman, W. S., Crespín, M., Cirillo, A. C., Abdo, S., Hall, W. K., *J. Catal.* **60**, 404 (1979).
7. Kim, S. I., and Woo, S. I., *J. Catal.* **133**, 124 (1992).
8. DeCanio, E. C., Edwards, J. C., Scalzo, T. R., Storm, D. A., and Bruno, J. W., *J. Catal.* **132**, 498 (1991).

9. (a) Tanabe, K., "Solid Acids and Bases," Academic Press, New York, 1970; (b) Kung, M. C. and Kung, H. H., *Catal. Rev.-Sci. Eng.* **27**, 425 (1985).
10. (a) Tanabe, K., in "Catalysis by Acids and Bases" (B. Imelik, C. Naccache, G. Coudurier, Y. Ben Taarit, and J. C. Vedrin, Eds.), Vol. 20, p. 1. Elsevier, Amsterdam, 1985; (b) Benesi, H. A. and Winquist, B. H. C., in "Advances in Catalysis" (D. D. Ely, H. Pines, and P. B. Weisz, Eds.), Vol. 27. Academic Press, New York, 1978.
11. Tanabe, K., Misono, M., Ono, Y., and Hattori, H., "New Solid Acids and Bases," Vol. 51. Elsevier, Amsterdam, 1989.
12. Hall, W. K., in "Proceedings, 4th International Conference on the Chemistry and Uses of Molybdenum," p. 244. Climax Molybdenum Co., Ann Arbor, Mich., 1982.
13. DeCanio, E. C., Bruno, J. W., Nero, V. P., and Edwards, J. C., *J. Catal.* **140**, 84 (1993).
14. Datka, J., *J. Chem. Soc., Faraday Trans. 1* **76**, 2437 (1980).
15. Hunger, M., Freude, D., and Pfeifer, H., *J. Chem. Soc. Faraday Trans.* **87**(4), 657 (1991).
16. Zamarayev, K. I., and Mastikhin, V. M., *Colloids Surf.* **12**, 401 (1984).
17. Engelhardt, G., and Michel, D., "High-Resolution Solid-State NMR of Silicates and Zeolites." Wiley, New York, 1987.
18. Pfeifer, H., Freude, D., and Hunger, M., *Zeolites* **5**, 274 (1985).
19. Reddy, B. M., and Mastikhin, V. M., in "Proceedings, 9th International Congress on Catalysis, Calgary, 1988" (M. J. Phillips, and M. Ternan, Eds.), Vol. 1, p. 82. Chem Inst. Canada, Ottawa, 1988.
20. Mastikhin, V. M., and Nosov, A. V., *React. Kinet. Catal. Lett.* **46**(1), 1239 (1992).
21. Mastikhin, V. M., Mudrakovskii, I. L., Kotsarenko, N. S., Karachiev, L. G., Pelmenchikov, and Zamarayev, K. I., *React. Kinet. Catal. Lett.* **27**(2), 447 (1985).
22. Engelhardt, G., Jerschke, H.-G., Lohse, U., Sarv, P., Samson, A., and Lippmaa, E., *Zeolites* **7**, 289 (1987).
23. Harris, R. K., "Nuclear Magnetic Resonance Spectroscopy: A Physicochemical View," p. 81. Longman, Avon, 1986.
24. Gerstein, B. C., *Adv. Colloid Interface Sci.* **23**, 45 (1985).
25. Böhm, J., Fenzke, D., and Pfeifer, H., *J. Magn. Reson.* **55**, 197 (1983).
26. Hunger, M., Freude, D., Pfeifer, H., Bremer, H., Jank, M., and Wendlandt, K.-P., *Chem. Phys. Lett.* **100**, 29 (1983).
27. Bronnimann, C. E., Chaung, I. S., Hawkin, B. L., and Maciel, G. E., *J. Am. Chem. Soc.* **109**, 1562 (1987).
28. Peri, J. B., *J. Phys. Chem.* **69**, 211 (1965).
29. Peri, J. B., *J. Phys. Chem.* **69**, 220 (1965).
30. Peri, J. B., *J. Phys. Chem.* **70**, 3168 (1966).
31. Choudhury, V. R., *Ind. Eng. Chem., Prod. Res. Dev.* **16**, 12 (1977).
32. Ghosh, A. K., and Kydd, R. A., *Catal. Rev.-Sci. Eng.* **27**(4), 539 (1985).
33. (a) Finch, J. N., and Clark, A., *Catal. Rev.-Sci. Eng.* **19**, 292 (1970); (b) Damon, J. P., Bonnier, J. M., and Delmon, B., *Bull. Chim. Soc. Fr.*, 449 (1975).
34. Allenger, V. M., McLean, D. D., and Ternan, M., *J. Catal.* **131**, 305 (1991).
35. (a) Webb, A. N., *Ind. Eng. Chem.*, 261 (1956); (b) Sockart, P. O., and Rouxhet, P. G., *J. Colloid Interface Sci.* **86**, 96 (1982).
36. Stanislaus, A., Absi-Halabi, M., and Al-Dolama, K., *Appl. Catal.* **39**, 239 (1988).
37. Morales, A., Ramirez De Argudelo, M. M., and Hernandez, F., *Appl. Catal.* **41**, 261 (1988).
38. O'Young, C.-L., Yang, C.-H., DeCanio, S. J., Patel, M. S., and Storm, D. A., *J. Catal.* **113**, 307 (1988).
39. Mastikhin, V. M., Mudrakovsky, I. L., and Nosov, A. V., *Prog. NMR Spectrosc.* **23**, 259 (1991).
40. Dean, J. A. "Langes Handbook of Chemistry," 13th ed., p. 5. McGraw-Hill, New York, 1985.
41. Fitz, C. W., and Rase, H. F., *Ind. Eng. Chem. Prod. Res. Dev.* **22**, 40 (1983).